# A Theoretical Investigation of the Magnetic and Ground-State Properties of Model Oxyhemoglobin Complexes

**Zelek S. Herman* and Gilda H. Loew***

*Contribution from the Department of Genetics, Molecular Theory Laboratory, Stanford University Medical Center, Stanford, California 94305.*
*Received May 10, 1979*

**Abstract:** Semiempirical INDO-SCF-CI calculations were made on a model oxyheme complex to determine the nature and relative energies of the ground and low-lying excited states. As a result of extensive configuration interaction, a singlet diamagnetic ground state is obtained with a very low-lying paramagnetic triplet ~150 $cm^{-1}$ above it. These results explain the temperature-dependent magnetic susceptibility recently observed in intact oxyhemoglobin. An antiferromagnetic singlet previously proposed as the ground state is found to be a highly excited state. The diamagnetic ground state has considerable $Fe^{III}(d^5)$–$O_2^-$ character due to extensive charge delocalization but does not involve transfer of spin density. The electric field gradient and quadrupole splitting calculated for this state are in excellent agreement with experiment for both the model oxyheme and the intact protein. The barrier to rotation of the terminal oxygen about the Fe–O bond was also calculated. A symmetric, fourfold barrier of 7.0 kcal/mol was obtained with the four minima bisecting the $N_{pyr}$–Fe–$N_{pyr}$ angles, consistent with the observed disorder in the crystal structure of the model compound.

## Introduction

The magnetic properties and electronic structure of oxyhemoglobin have attracted the attention of researchers for nearly half a century. In 1936, Pauling and Coryell[1] measured the magnetic moment at 20 °C of oxyhemoglobin in blood and in solution and found that oxyhemoglobin is diamagnetic at this temperature, corresponding to an electronic structure in which all the electrons in each heme group are spin paired. The conclusion that, in solution at 20 °C, oxyhemoglobin is diamagnetic was verified for cow oxyhemoglobin by Coryell et al.[2] and for horse, sheep, and human hemoglobin by Taylor and Coryell.[3] This observation was accepted for 40 years until, in 1977, Cerdonio et al.[4] reported measurements for the magnetic susceptibility of frozen aqueous solutions of human oxyhemoglobin in the temperature range 25–250 K. They found a temperature-dependent behavior typical of a thermal equilibrium between a ground singlet state and an excited triplet state having two unpaired electrons per heme group, with an energy separation between these two states of 146 $cm^{-1}$. In a published rebuttal[5] of the conclusions reached by Cerdonio and co-workers, Pauling attributed the paramagnetism they observed in frozen samples to partial dissociation of oxygen. Subsequently, Cerdonio et al.[6] published new results on the magnetic susceptibilities at room temperature of oxyhemoglobin and of carbonmonoxyhemoglobin solutions of various concentrations. These findings confirm their earlier results for frozen solutions and seem to dispel Pauling's rebuttal. Despite this intense experimental effort, the matter still has not been completely resolved.

In addition to the enigma of whether oxyhemoglobin has any low-lying states with unpaired spins which could account for the observed paramagnetism in the above temperature range, there exists also the outstanding question concerning the nature of such states and of the ground state as well. Both the earlier and more recent magnetic measurements are consistent with no net unpaired spins in the lowest lying state of oxyhemoglobin. However, because of similarities between the electronic spectra of oxyhemoglobin and alkaline metmyoglobin[7-10] and the anomalously large quadrupole splitting in the Mössbauer spectra of intact protein and model compounds,[11] it has been suggested that the ground state, rather than being diamagnetic, involves an electron transfer from the iron atom to the oxygen moiety, leading to an "antiferromagnetic" state, a term borrowed from a solid-state phenomenon. On a molecular level, this concept has been employed in the case of oxyhemoglobin to denote a spin-paired biradical of the type $Fe^{III}(d^5\uparrow)$–$O_2^-(\downarrow)$ rather than the $Fe^{II}(d^6)$–$O_2$ diamagnetic description of the ground state, as originally proposed by Pauling.[12]

If the reported temperature-dependent magnetic susceptibility is correct, there should be a low-lying triplet state which could correspond either to the "ferromagnetic" partner of an "antiferromagnetic" ground state or to any low-energy paramagnetic triplet state in thermal equilibrium with a diamagnetic ground state. The temperature-dependent susceptibility data alone cannot distinguish between these two possibilities since the data can be fit to either model.

A number of theoretical calculations,[13-24] both semiempirical and ab initio, have been reported for model compounds in order to elucidate the electronic structures of oxyhemoglobin. However, none of these studies has shown conclusively whether the ground state is diamagnetic or a spin-paired biradical (antiferromagnetic) and whether the bonding of the dioxygen to the heme can be described better by a $Fe^{II}$–$O_2$ formulation or $Fe^{III}$–$O_2^-$ formulation.[19-22] Furthermore, none of the theoretical studies has addressed the question of the presence of low-lying triplets and singlets by utilizing the method of configuration interaction, although Dedieu et al.[18] do suggest that, were one to perform configuration-interaction calculations, one would probably find an excited triplet state lying close in energy to a diamagnetic ground state.

In order to more definitively characterize both the ground and low-lying excited states of oxyheme proteins, we have performed LCAO-MO-SCF-CI calculations on a model for the active oxyhemoglobin, using a newly developed INDO-type (intermediate neglect of differential overlap)[25] program which includes transition metals and extensive configuration interaction involving single and double excitations. The results of these calculations give the relative energies and electron distributions in the ground and excited states and are consistent with the observed temperature-dependent magnetic susceptibility.[11,26,27]

For the ground electronic state, the electric field gradient at the iron nucleus and the resulting quadrupole splitting have been calculated as a function of rotation of the terminal oxygen atom about the Fe–O bond. The crystallographic data for

* Molecular Theory Laboratory, 701 Welch Rd., The Rockefeller University, Palo Alto, Calif. 94304.

0002-7863/80/1502-1815$01.00/0 

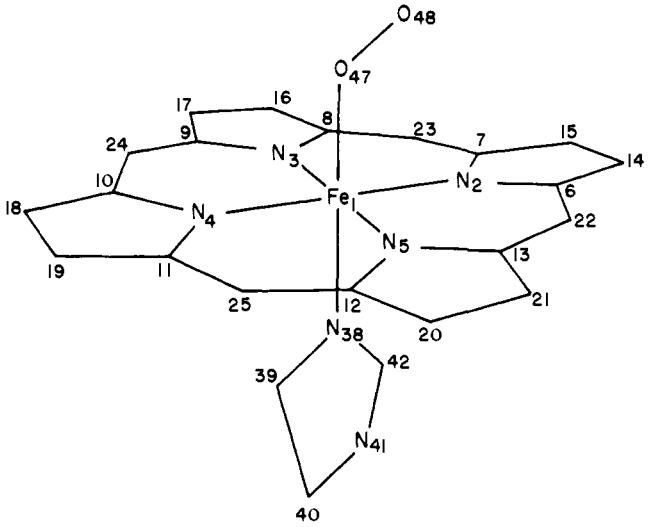


**Figure 1.** Model oxyheme showing the coordinate and numbering systems of heavy atoms. Unless noted otherwise, all numbers refer to carbon atoms. Relevant interatomic distances are $Fe_1$–$N_{38}$ (2.06 Å); $Fe_1$–$N_{pyrrole}$ (2.01 Å); $O_{47}$–$O_{48}$ (1.23 Å). The angle Fe–O–O is 135°. The imidazole ring lies at an angle of 67.5 from the line $Fe_1$–$C_{22}$.

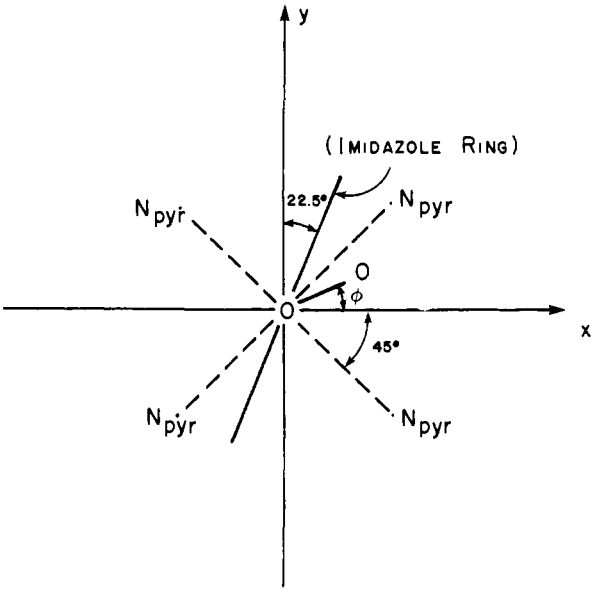


**Figure 2.** Relative orientation of the axial ligands $O_2$ and imidazole projected onto the porphyrin plane in model oxyheme. The value of $\phi$ ($C_{22}$–Fe–O–O) = 0° corresponds to the $O_2$ ligand bisecting the ($N_{pyr}$–Fe–$N_{pyr}$) bond angle and is the conformer used in the configuration-interaction calculations.

model compounds of oxyhemoglobin indicate a large disorder and consequent ambiguity in the position of the second oxygen atom due to rotations about the iron–oxygen bond.[28-30] The barrier to such rotation of the dioxygen ligand has also been calculated.

## Method

The calculations were performed using a recently developed INDO program[31-34] which allows for the treatment of transition-metal complexes and the inclusion of extensive configuration interaction. This program has been successfully applied to describe the ground state and/or spectral properties of $[FeCl_4]^-$, $[CoCl_4]^{2-}$, $[CuCl_4]^{2-}$,[33,34] oxy-$P_{450}$ and carboxy-$P_{450}$,[35] and ferrocene.[36] A characteristic feature of this program is that it includes the evaluation of all one-center exchange terms necessary for rotational invariance. The program includes options for both theoretical and empirical evaluation of the two-center repulsion integrals, the latter employing an empirical Weiss–Mataga–Nishimoto formula.[37,38] The empirical parametrization is based on optimizing the two-electron integrals to yield good spectral results for a series of model compounds and involves some degree of relaxation, whereas the theoretical parametrization involves the theoretical calculation of the two-electron integrals over atomic orbitals whose exponents have been optimized in order to parallel not only the eigenvalues and eigenvectors of ab initio calculations for a series of model compounds but the experimentally observed dipole moments and equilibrium geometries as well.[33] In order to guarantee convergence for systems containing transition metals with specific configurations, the program allows for specifying the occupancy of the metal d orbitals. This program has been successfully applied to describe the electronic structure of many transition-metal systems.[33,34] More recently, the program has been utilized to calculate the electronic spectrum of ferrocene, yielding good agreement with the experimentally observed spectral transitions.[36]

The model employed for the oxyferroheme protein is a regularized version of the model oxyheme complex synthesized by Collman and co-workers.[30,39] As shown in Figure 1, the model consists of a planar porphyrin ring and two axial ligands, imidazole and dioxygen. The dioxygen bisects the two adjacent pyrrole nitrogens ($\phi$ = 0° in Figure 2) while the imidazole ring makes a 22.5° angle with the $y$ axis (Figure 2). Previous calculations[16,18,19] have shown that the $\phi$ = 0° conformer is one of the lowest energy rotational conformers and that the bent (Pauling[40]) structure is substantially more stable than the perpendicular (Griffith[41]) structure. Thus, the Pauling structure with the X-ray values for the bond length, bond angle, and torsion angle of the Fe–$O_2$ group was chosen for the major part of this study, together with the X-ray conformation of the imidazole ring. The barrier to rotation about the Fe–O axis and the effect of this rotation on calculated values of the electric field gradient at the iron nucleus were also determined.

The investigation of the model oxyheme complex was initiated with SCF–MO–LCAO level calculations invoking the assignment of electrons to d orbitals in order to ensure convergence to a formal $Fe^{II}$ $d^6$ ($S$ = 0) state. These calculations were performed using the new INDO program with both the theoretical and empirical parametrizations. A possible lowering in energy of this closed-shell diamagnetic state by configuration interaction was then explored. For this purpose, a symmetry analysis of the eigenvectors resulting from these SCF calculations, both for the theoretical and for the spectroscopic parametrization developed specifically for optimum CI results, was made assuming an approximate $C_{2v}$ symmetry for the iron and $D_{4h}$ symmetry for the porphyrin group, when appropriate in the overall molecular symmetry of $C_1$.

Using the symmetry analysis as a guide, a set of doubly excited configurations of appropriate symmetry was selected to interact with the SCF closed-shell configurations. Since the INDO program allows for simultaneous interaction of a maximum of 115 configurations, a strategy was adopted whereby an initial set of configurations thought to be important was selected. Those configurations which did not contribute significantly to the ground state were eliminated, and others were added until nearly the whole manifold of occupied orbitals and all the important virtual orbitals were explored. A final 115-dimensional CI calculation was then made with all the important excitations selected from some 600 configurations explored in this iterative process.

A similar configuration-interaction procedure was followed to investigate the energy of candidate excited singlet and triplet states which could correspond to molecular "antiferromagnetic", "ferromagnetic", or paramagnetic states. Excited singlet states, formed by transfer of an electron from orbitals containing significant d character to orbitals containing sig-

nificant Oπ character, were included in an extensive configuration-interaction calculation designed to lower the energy of such "antiferromagnetic" (spin-paired singlet) states competitively with the diamagnetic singlet state. In these configuration interaction calculations, *all* singly and doubly excited states which mixed significantly with such singlet states were included by an iterative CI procedure similar to that employed for the diamagnetic state. Almost the entire manifold of occupied and all important virtual orbitals were again systematically included in these calculations.

The energies of excited triplet states corresponding to paramagnetic states with spin density on both the iron and the dioxygen ligand in various degrees of delocalization were also calculated by the method of configuration interaction, this time including a triplet manifold connected only by single excitations from candidate triplet states.

The aim of these extensive configuration interaction calculations was to obtain a reliable energy ordering of the lowest diamagnetic, antiferromagnetic, and triplet (paramagnetic) states.

For the lowest energy state, the electronic distribution, i.e., iron–ligand bonding and extent of delocalization (covalency), was investigated using a Mulliken population analysis[42] of the SCF eigenvectors. Even for a closed-shell ground state, the electron distribution could correspond to either a $Fe^{III}(d^5)$-$O_2^-$ or a $Fe^{II}(d^6)$-$O_2$ description of the complex.

To determine the reliability of electronic distributions obtained from the INDO-SCF procedure with theoretical and empirical parametrization, a ground-state property which is very sensitive to the electron distribution, namely, the electric field gradient at the iron nucleus, was calculated employing the eigenvectors resulting from both parametrizations. The empirical parametrization was found to yield electric field gradients and quadrupole splittings in excellent agreement with those observed in intact oxyheme proteins and the model compound, whereas the results from the theoretical parametrization were in complete disagreement with experiment. Therefore, the SCF eigenvectors resulting from the empirical parametrization were chosen as a more reliable description of electron distribution, bonding, and covalent delocalization in the model oxyheme.

The INDO-SCF procedure with empirical parametrization was also used to calculate the barrier to rotation of the terminal oxygen about the Fe-O bond with no other geometry relaxation, as well as the electric field gradients and quadrupole splittings as a function of this rotation. These results were utilized to account for the rotational disorder of $O_2$ ligand observed in the model compound and the observed temperature dependence of the quadrupole splitting in the Mössbauer resonance spectra.

## Results

The lowest energy states for the model oxyheme obtained after extensive configuration interaction calculations are given in Figure 3. All energies are relative to the CI results for the diamagnetic ground state which was lowered by 10 626 $cm^{-1}$. The salient feature of this energy diagram is that the ground state ($a^1A$) is diamagnetic and is separated from the lowest energy triplet state ($a^3A$) by only 129 $cm^{-1}$. This triplet state is best described as a normal paramagnetic state.

The lowest lying "antiferromagnetic" singlet state involving excitation from a molecular orbital containing significant d character to an orbital containing significant Oπ character is 13 500 $cm^{-1}$ above the diamagnetic ground state and above two other low-lying triplet states. Our results clearly rule out such a state as the ground state. It should be pointed out, however, that this singlet calculated to be 13 500 $cm^{-1}$ above the ground state may not be the lowest excited singlet state; in fact, two singlet states at about 10 000 $cm^{-1}$ have been found[23,43] in the single-crystal polarized absorption spectra of oxyhemoglobin and oxymyoglobin. Calculations[44] of the electronic spectrum of model oxyheme indicate that these transitions can be assigned to singlet states which involve prophyrin $\pi \rightarrow (d\pi\text{-}O\pi)^*$ excitations. Even these types of charge transfer singlet states are still too far above the diamagnetic ground state to be of relevance for the magnetic properties of oxyhemoglobin.

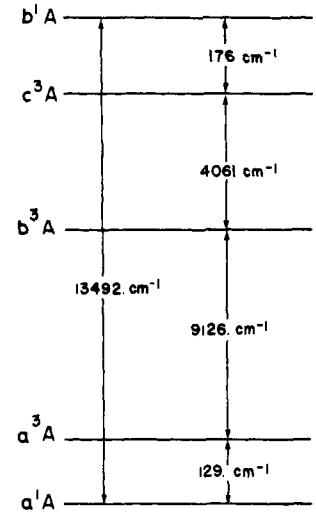


**Figure 3.** Energies of the lowest triplet and singlet excited states of model oxyheme resulting from the SCF–CI calculations with empirical parametrization. All energies are relative to the diamagnetic ground state $^1A$. The excited $b^1A$ state is the lowest energy "antiferromagnetic" singlet state. All triplet states are paramagnetic states.

Without CI, a totally different energy ordering is obtained. In the SCF energy ordering, the paramagnetic $a^3A$ state is the ground state, with the diamagnetic singlet $a^1A$ state and the excited antiferromagnetic singlet state $b^1A$ 1754 and 15 370 $cm^{-1}$ above it, respectively. Configuration interaction lowers all of these states significantly, but by different amounts: the $a^3A$ state by 8743 $cm^{-1}$, the $a^1A$ (diamagnetic) ground state by 10 626 $cm^{-1}$, and the $b^1A$ (antiferromagnetic) state by 10 751 $cm^{-1}$, resulting in the order shown in Figure 3. These quantitative differences in the SCF and CI results indicate the importance of configuration interaction in determining the relative energies of the ground and low-lying excited states in model heme systems.

Tables I and II describe the important configurations contributing to the diamagnetic ground state and the lowest lying triplet and singlet states. The nature of the molecular orbitals obtained from the SCF calculation with empirical parametrization is given in Table I. In Table II, the most important configurations in each of these three states are presented. The major configuration in the lowest energy triplet states are the single excitations 77→80 (77%) and 77→82 (13%). Examining the orbitals in Table I, we see that these excitations correspond to the following electron transfers: $(d_{yz}\text{-}O\pi) \rightarrow (O\pi\text{-}d_{yz})^*$ and $(d_{yz}\text{-}O\pi) \rightarrow$ porphyrin $\pi^*$ ($e_g$), respectively.

In Table III, the bond overlap densities and net atomic charges for the diamagnetic ground state of the model oxyheme, calculated from a Mulliken population analysis, are displayed for both the empirically and theoretically parametrized INDO results as well as the ab initio results of Dedieu et al.[18] The atomic populations for the iron, oxygen, and pyrrole and imidazole nitrogen atoms are given in Table IV.

The quadrupole splitting $\Delta E_Q$ observed in Mössbauer resonance of the heme compound was also calculated employing the INDO-SCF eigenvectors from both the empirical and theoretical parametrizations. This quantity was determined by first calculating the nine components $V_{ij}$ of the electric field

**Table I.** INDO (Empirical Parametrization) Eigenvalues and Eigenvectors for Model Oxyheme

| MO[a] | orbital energy, au | symmetry[b] | principal atomic orbital coefficients[c] | % Fe | % O |
|---|---|---|---|---|---|
| 88 | 0.053 | $b_{1u}$ | $\pm0.25N_{2\text{-}5}p_z \pm0.28C_{6\text{-}13}p_z \pm0.12C_{14\text{-}21}p_z$ | 0 | 0 |
| 87 | 0.044 | $a_1$; $a_2$ | $+0.61d_{z^2} -0.49d_{xy} +0.21N_{2,4}s -0.20N_{38}s -0.12O_{47}p_x +0.16O_{47}p_z -0.11O_{48}p_z$ | 62 | 6 |
| 86 | 0.040 | $a_1$; $a_2$ | $+0.47d_{z^2} +0.62d_{xy} +0.21N_{3,5}s +0.15N_{38}s +0.13O_{47}p_z$ | 61 | 4 |
| 85 | 0.038 | imidazole $\pi$ | $-0.32N_{38}p_x +0.13N_{38}p_y +0.64C_{39}p_x -0.27C_{39}p_y -0.54C_{40}p_x +0.22C_{40}p_y +0.12N_{41}p_x +0.14C_{42}p_x$ | 2 | 0 |
| 84 | 0.012 | $b_{2u}$ | $\pm0.11C_{6\text{-}13}p_z \pm0.26C_{14\text{-}21}p_z \pm0.30C_{22\text{-}25}p_z$ | 0 | 0 |
| 83 | −0.002 | imidazole $\pi$ | $-0.39N_{38}p_x +0.16N_{38}p_y +0.30C_{40}p_x -0.13C_{40}p_y -0.39C_{41}p_x +0.16C_{41}p_y +0.67C_{42}p_x -0.28C_{42}p_y$ | 0 | 0 |
| 82 | −0.047 | $b_2$; $O\pi_g{}^b$; $e_g$ | $-0.35d_{yz} \pm0.16N_{2\text{-}5}p_z \pm0.24C_{6,9,10,13}p_z \pm0.10C_{14,17,18,21}p_z \pm0.22C_{13,15,16,19,20}p_z \pm0.34C_{23,25}p_z +0.18O_{47}p_y -0.15O_{48}p_y$ | 12 | 5 |
| 81 | −0.051 | $e_g$ | $\pm0.16N_{2\text{-}5}p_z \pm0.28C_{7,8,11,12}p_z \pm0.10C_{15,16,19,20}p_z \pm0.24C_{14,17,18,21}p_z \pm0.36C_{22,24}p_z$ | 1 | 0 |
| 80 | −0.071 | $b_2$; $O\pi_g{}^b$ | $-0.60d_{yz} \pm0.15C_{6,9,10,13}p_z \pm0.11C_{15,16,19,20}p_z +0.49O_{47}p_y -0.43O_{48}p_y$ | 36 | 43 |
| 79 | −0.239 | $a_{1u}$ | $\pm0.31C_{6\text{-}13}p_z \pm0.16C_{14\text{-}21}p_z$ | 0 | 0 |
| 78 | −0.255 | $a_{2u}$ | $+0.24N_2\text{-}N_5 +0.13C_{14\text{-}21}p_z -0.38C_{22\text{-}25}p_z$ | 0 | 0 |
| 77 | −0.292 | $b_2$; $O\pi_g{}^b$; porphyrin $\pi$ | $-0.55d_{yz} \pm0.14N_{2\text{-}5}p_z \pm0.10C_{6,9,10,13}p_z \pm0.11C_{15,16,17,19,20,21}p_z -0.34O_{47}p_y +0.59O_{48}p_y$ | 32 | 47 |
| 76 | −0.320 | $b_1$; $O\pi_g{}^a$; porphyrin $\pi$ | $-0.11d_{z^2} +0.58d_{xz} \pm0.23N_{2\text{-}5}p_z \pm0.10C_{7,8,11,12} \pm0.15C_{14\text{-}19,21}p_z -0.22O_{47}p_x +0.17O_{47}p_z +0.28O_{48}p_x -0.21O_{48}p_z$ | 35 | 21 |
| 75 | −0.335 | $O\pi_g{}^a$; porphyrin $\pi$ | $-0.12d_{z^2} -0.10d_{xz} +0.25N_{2,5}p_z -0.13N_4p_z -0.20C_{14,15,20,21}p_z -0.33O_{47}p_x +0.29O_{47}p_z +0.45O_{48}p_x -0.42O_{48}p_z$ | 3 | 58 |
| 74 | −0.345 | $b_{1u}$; imidazole $\pi$ | $\pm(0.19\text{-}0.32)N_{2\text{-}5}p_z \pm(0.16\text{-}0.29)C_{14\text{-}21}p_z +0.20C_{39}p_x +0.24C_{40}p_x -0.11C_{40}p_y -0.20C_{42}p_x$ | 0 | 0 |
| 73 | −0.350 | $a_{2u}$ | $+(0.21\text{-}0.34)N_{2\text{-}5}p_z \pm(0.21\text{-}0.31)C_{14\text{-}21}p_z +0.09O_{47}p_x -0.19O_{48}p_x +0.15O_{48}p_z$ | 1 | 7 |
| 72 | −0.355 | $b_{1u}$; imidazole $\pi$ | $-0.12d_{xz} \pm(0.14\text{-}0.22)N_{2\text{-}4}p_z \pm0.18C_{14\text{-}19}p_z -0.20N_{38}p_x +0.38C_{39}p_x -0.17C_{39}p_y +0.47C_{40}p_x -0.19C_{40}p_y -0.39C_{42}p_x +0.17C_{42}p_y$ | 2 | 2 |
| 71 | −0.359 | $b_2$; $e_g$ | $0.17d_{yz} \pm0.13N_{2\text{-}5}p_z \pm0.19C_{6,7,10,11}p_z \pm0.27C_{14,16,17,18,20,21}p_z \pm(0.10\text{-}24)C_{22\text{-}25}p_z -0.13C_{39,40}p_x -0.17O_{48}p_y$ | 4 | 3 |
| 70 | −0.361 | $e_g$ | $\pm(0.15\text{-}0.25)C_{6\text{-}13}p_z \pm(0.15\text{-}0.25)C_{13\text{-}20}p_z \pm0.36C_{22,24}p_z$ | 1 | 1 |
| 69 | −0.363 | $a_1$, $b_2$; $e_g$ | $-0.37d_{x^2-y^2} -0.23d_{yz} \pm0.23N_{2\text{-}5}p_z \pm0.16C_{6\text{-}13}p_z \pm0.11C_{15,16,19,20}p_z \pm0.32C_{23,25}p_z +0.13C_{39}p_x +0.21O_{48}p_y$ | 20 | 5 |
| 68 | −0.364 | $a_1$; $e_g$ | $-0.87d_{x^2-y^2} +0.14d_{yz} \pm0.11N_{2\text{-}5}p_z \pm0.11C_{23,25}p_z -0.11O_{48}p_y$ | 78 | 2 |
| 67 | −0.387 | $b_1$ | $-0.69d_{xz} \pm0.17N_{2\text{-}5}p_z \pm0.11C_{14\text{-}21}p_z \pm0.12C_{22,24}p_z -0.18N_{38}p_x -0.20C_{40}p_x +0.20N_{41}p_x +0.16O_{48}p_x -0.26O_{48}p_z$ | 48 | 10 |

[a] Molecular orbitals 1–79 are doubly occupied; MOs 80 and above are virtual orbitals. [b] The actual symmetry of the molecule is $C_1$. Irreducible representation labels from $C_{2v}$ and $D_{4h}$ are employed to denote the iron and porphyrin groups, respectively. $O\pi_g{}^a$ and $O\pi_g{}^b$ denote the oxygen $\pi$ orbitals in the $xz$ and $yz$ planes, respectively. [c] The atoms are numbered as in Figure 1. The coefficients are averaged, where appropriate, in order to display the approximate symmetry. For example, $\pm0.19C_{6,7,10,11}p_z$ refers to the average coefficients of the $p_z$ atomic orbital centered on carbon atoms 6, 7, 10, and 11.

**Table II.** Symmetry Classification of the Five Most Important Configurations in Each of the CI Calculations

| state | configuration[a] | coefficient in CI | symmetry classification[b] |
|---|---|---|---|
| diamagnetic ground state | (77,77)→(80,80) | −0.343 | $(b_2(d_{yz}),O\pi_g{}^b)\rightarrow(O\pi_g{}^b,b_2(d_{yz}))^*$ |
| | (69,77)→(80,80) | 0.108 | |
| | (71,77)→(80,80) | −0.089 | |
| | (68,77)→(80,80) | −0.059 | |
| | (72,72)→(83,83) | 0.062 | imidazole $\pi\rightarrow\pi^*$ |
| lowest excited triplet state | 77→80 | 0.879 | $(b_2(d_{yz}),O\pi_g{}^b)\rightarrow(b_2(d_{yz}),O\pi_g{}^b)^*$ |
| | 71→80 | −0.155 | |
| | 77→82 | 0.355 | $(b_2(d_{yz}),O\pi_g{}^b,e_g)\rightarrow(b_2(d_{yz}),O\pi_g{}^b,e_g)^*$ |
| | 69→80 | 0.188 | $b_2(d_{yz})\rightarrow b_2{}^*(d_{yz})$ |
| | 68→80 | 0.095 | |
| lowest excited antiferromagnetic singlet state | 76→80 | 0.775 | $(b_1(d_{xz}),O\pi_g{}^a)\rightarrow(b_2(d_{yz}),O\pi_g{}^b)^*$ |
| | 67→80 | −0.250 | |
| | 76→82 | 0.316 | $(b_1(d_{xz}),O\pi_g{}^a,e_g)\rightarrow(b_2(d_{yz}),O\pi_g{}^b,e_g)^*$ |
| | 67→82 | −0.132 | |
| | 75→80 | 0.379 | $O\pi_g{}^a\rightarrow O\pi_g{}^{b\,*}$ |

[a] The notation $(i,j)\rightarrow(a,b)$ refers to the double excitation of an electron from occupied orbital $i$ and another electron from occupied orbital $j$ to the virtual orbitals $a$ and $b$. $i\rightarrow a$ represents the single excitation of an electron from occupied orbital $i$ to the virtual orbital $a$. [b] Same notation as in Table I.

gradient tensor, using the appropriate one-electron operator, and considering only the contribution of the iron from all its filled orbitals. The 3 × 3 electric field gradient tensor was then diagonalized and the principal values ordered: $|V_{ii}| > |V_{jj}| > |V_{kk}|$. These values were then used in the expression

$$\Delta E_Q = 8(1 - R)Qq[1 + \eta^2/3]^{1/2}$$

where $q = V_{ii}$, $\eta = (V_{kk} - V_{jj})/V_{ii}$ $(0 \le \eta < 1)$, $(1 - R) =$

**Table III.** Calculated Bond Overlap Densities and Net Atomic Charges for the Model Oxyheme

| property | empirical $\gamma$ | theoretical $\gamma$ | ab initio[a] |
|---|---|---|---|
| bond overlap[b] | | | |
| Fe–$O_{47}$ | 0.48 | 0.40 | |
| $O_{47}$–$O_{48}$ | 0.56 | 0.62 | |
| Fe–$N_{pyrrole}$ | 0.46 | 0.47 | |
| Fe–$N_{imidazole}$ | 0.42 | 0.42 | |
| net charges[b] | | | |
| Fe | 1.41 | 0.80 | 1.23 |
| $O_{47}$ | −0.27 | −0.05 | −0.04 |
| $O_{48}$ | −0.48 | −0.03 | +0.07 |
| $N_{pyrrole}$ | 0.47 | 0.35 | |
| $N_{imidazole}$ | 0.41 | 0.22 | |

[a] Valence contribution estimated by subtracting the contribution of fully occupied core orbitals from the reported total orbital populations (ref 18). [b] Calculated from a Mulliken population analysis.

**Table IV.** Atomic Populations for the Iron, Oxygen, and Pyrrole and Imidazole Nitrogen Atoms in the Model Oxyheme as Calculated from a Mulliken Population Analysis

| atomic orbital | empirical $\gamma$ | theoretical $\gamma$ | ab initio[a] |
|---|---|---|---|
| Fe 4s | 0.16 | 0.25 | 0.15 |
| $4p_x$, $4p_y$ | 0.14 | 0.24 | 0.11 |
| $4p_z$ | 0.09 | 0.11 | 0.07 |
| $3d_{z^2}$ | 0.57 | 0.22 | 0.22 |
| $3d_{x^2-y^2}$ | 1.98 | 2.00 | 1.91 |
| $3d_{xy}$ | 0.55 | 0.28 | 0.33 |
| $3d_{xz}$ | 1.96 | 1.98 | 1.96 |
| $3d_{yz}$ | 1.01 | 1.89 | 1.90 |
| $O_{47}$ 2s | 1.88 | 1.92 | 1.80 |
| $2p_x$ | 1.54 | 1.56 | 1.36 |
| $2p_y$ | 1.44 | 1.05 | 1.36 |
| $2p_z$ | 1.41 | 1.52 | 1.53 |
| $O_{48}$ 2s | 1.93 | 1.93 | 1.87 |
| $2p_x$ | 1.50 | 1.52 | 1.27 |
| $2p_y$ | 1.59 | 1.06 | 1.27 |
| $2p_z$ | 1.46 | 1.52 | 1.53 |
| $N_{pyrrole}$ 2s | 1.65 | 1.54 | |
| $2p_x$ | 1.13 | 1.15 | |
| $2p_y$ | 1.13 | 1.15 | |
| $2p_z$ | 1.56 | 1.51 | |
| $N_{imidazole}$ 2s | 1.68 | 1.56 | |
| $2p_x$ | 1.36 | 1.26 | |
| $2p_y$ | 1.13 | 1.11 | |
| $2p_z$ | 1.25 | 1.29 | |

[a] Valence electron contribution estimated by subtracting the contribution of fully occupied core orbitals from the reported orbital populations (ref 18). Note that, because they employed a different coordinate system, the iron $d_{x^2-y^2}$ orbital of ref 18 corresponds to our $d_{xy}$ orbital.

Sternheimer shielding constant, and $Q$ = nuclear quadrupole moment. The sign of $\Delta E_Q$ is the sign of the largest component $V_{ii}$ and $(1 - R)Q = 0.127$, consistent with the most recent estimate of these quantities.[45] These calculations yielded values of $\Delta E_Q$ equal to −2.16 mm/s for the empirical parametrization, in excellent agreement with the "anomalously large" experimental low-temperature value of $\Delta E_Q = -2.10$ mm/s in the model oxyheme complex.[26] By contrast a value of +0.54 mm/s was obtained from the theoretical parametrization. This result implies that the empirical parametrization, which is also more reliable in the configuration interaction calculation of the relative excited state energies, provides a much better description of the ground state than does the theoretical one.

As seen in Table III, the net charges on the iron and oxygen obtained from the empirically parametrized INDO-SCF results correspond more to an $Fe^{III}(d^5)$-$O_2^-$ description while those from the theoretical parametrization, and from the ab initio calculation as well, correspond more to an $Fe^{II}(d^6)$-$O_2$ complex with greatly reduced positive charge on the iron and nearly neutral oxygen atoms. The atomic populations in Table IV confirm these differences: the d-orbital population from the empirical parametrization is $(d_{x^2-y^2})^{1.98}(d_{xz})^{1.96}(d_{yz})^{1.01}$, whereas from the theoretical results it is $(d_{x^2-y^2})^{2.00}(d_{xz})^{1.98}(d_{yz})^{1.89}$.

**Table V.** Calculated Quadrupole Splittings ($\Delta E_Q$) for Various Rotational Conformers of Model Oxyheme

| $\phi$, deg | $\Delta E_q$, mm/s[a] | $\eta$ | largest component $V_{ii}$ |
|---|---|---|---|
| 0[b] | 0.54[c] | 0.40[c] | $V_{zz} = +0.52$[c] |
| 0 | −2.16 | 0.40 | $V_{xx} = -2.07$ |
| 22.5 | −2.20 | 0.40 | $V_{xx} = -2.10$ |
| 45 | −2.40 | 0.35 | $V_{xx} = -2.32$ |
| 67.5 | −2.61 | 0.38 | $V_{xx} = -2.51$ |
| 90 | −2.13 | 0.41 | $V_{yy} = -2.04$ |
| 135 | −2.48 | 0.31 | $V_{yy} = -2.40$ |
| 180 | −2.13 | 0.42 | $V_{xx} = -2.03$ |
| 247.5 | −2.62 | 0.38 | $V_{xx} = -2.51$ |
| 270 | −2.12 | 0.41 | $V_{yy} = -2.03$ |
| 315 | −2.48 | 0.30 | $V_{xx} = -2.40$ |

[a] Calculated from $\Delta E_Q = 8(1 - R)Qq[1 + \eta^2/3]^{1/2}$ with the principal axis values of the field gradient ordered $|V_{ii}| > |V_{jj}| > |V_{kk}|$. $q$ = largest magnitude $V_{ii}$ and the anisotropy $\eta = (V_{kk} - V_{jj})/V_{ii}$ $(0 \le \eta < 1)$. Sign of $\Delta E_Q$ is the sign of the largest component $V_{ii}(1 - R)$. For iron, $(1 - R)Q$ is taken as 0.127. [b] Value resulting from theoretical parametrization. All other values are from empirical parametrization. [c] These values agree with those calculated from the ab initio eigenvalues supplied by Dr. M.-M. Rohmer for Fe(Porph)-$O_2NH_3$, in which the $O_2$ has the same orientation. The ab initio values are: $\Delta E_Q = 0.52$, $\eta = 0.64$, $V_{zz} = +0.48$.

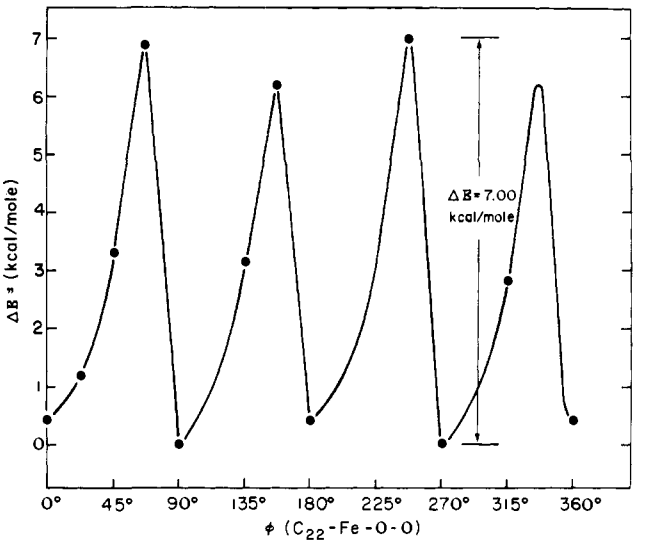


**Figure 4.** Calculated energy (kcal/mol) of rotation of the terminal oxygen atom about the $\phi$ ($C_{22}$–Fe–O) axis relative to lowest energy conformers.

The observed temperature dependence of the electric field gradient can have a number of origins. One possibility is that both the diamagnetic ground state and the lowest lying, paramagnetic triplet state contribute to the observed high-temperature value of $\Delta E_Q$. This possibility does not seem to be a likely source of temperature variation in the value of $\Delta E_Q$ since the calculated d-orbital coefficients, from which $\Delta E_Q$ is calculated, are virtually the same in these two states (see Tables I and II).

Another possible source of the observed temperature dependence of the electric field gradient could be rotation of the terminal oxygen atom about the Fe–O bond. The variation of the empirically parametrized INDO-SCF energy as a function of the Fe–O torsion angle is shown in Figure 4 while the corresponding calculated quadrupole splittings are tabulated in

**Table VI.** Comparison between Calculated and Observed Temperature Dependence of the Quadrupole Splitting of Oxyheme[j]

| | $\Delta E_Q$, mm/s | | $\eta$ | | largest component $V_{ii}$ | | $\Delta E_Q$(high $T$)/ |
|---|---|---|---|---|---|---|---|
| | low $T$ | high $T$ | low $T$ | high $T$ | low $T$ | high $T$ | $\Delta E_Q$(low $T$) |
| model | | | | | | | |
| obsd | −2.10[a] | 1.31[b] | $0.1 \leq \eta \leq 0.3$[a] | | | | 0.62 |
| calcd | −2.16[c] | 1.54[d] | 0.40[c] | 0.50[d] | $V_{xx} = -2.07$[c] | $V_{zz} = 1.45$[d] | 0.71 |
| protein | | | | | | | |
| obsd | −2.24[e] | −1.89[f] | $0.3 \leq \eta \leq 0.4$[g] | | $V_{xx}$ or $V_{yy}$[g] | | 0.84 |
| calcd | −2.20[h] | −2.18[i] | 0.40[h] | 0.41[i] | $V_{xx} = -2.10$[h] | $V_{xx} = -2.08$[i] | 0.99 |

[a] At $T = 4.2$ K (ref 26). [b] At $T = 195$ K (ref 26); sign of $\Delta E_Q$ not determined. [c] $\phi = 0°$. [d] Quantum average for $\phi = 0.45$, 67.5, 90, and 135°. [e] At $T = 1.2$ K (ref 26). [f] At $T = 195$ K; $\Delta E_Q = -2.19$ mm/s at $T = 77$ K (ref 26). Sign of $\Delta E_Q$ not determined. [g] Crystal measurement on oxymyoglobin (ref 27); principal value of $V_{ii}$ in heme plane. [h] $\phi = 22.5°$. [i] Quantum average for $\phi = 0$, 22.5, and 45°. [j] Notation is the same as for Table V.

Table V. The rotational barrier is seen to have a fully symmetric, fourfold barrier of about 7 kcal/mol. The result is consistent with the observed thermal disorder and fourfold symmetry in the position of the terminal oxygen in the model oxyheme complex.[39]

Inasmuch as low-energy rotation in the model compound appears possible at higher temperatures, contributions to the field gradient from all values of the torsion angle were included by averaging the nine components for the torsion angles of 0, 45, 67.5, 90, and 135°. This leads to a value of $\Delta E_Q = 1.54$ mm/s, in excellent agreement with the observed high-temperature value in the model compound. In oxyhemoglobin, the ligand pocket might not accommodate the large rotational variations possible in the model compound.[30,46] Therefore, one can simulate temperature dependence in the protein by averaging the nine components of the electric field gradient over the more restricted range of values of $\phi = 0$, 22.5, and 45° while the low-temperature value can be simulated by the single conformer with $\phi = 22.5°$. The temperature dependence of $\Delta E_Q$ obtained for the model compound and intact protein with these assumptions is summarized in Table VI and compared to the experimental observations.

## Discussion

The inclusion of extensive configuration interaction in the empirical INDO–SCF treatment of model oxyheme indicates that the ground state is diamagnetic and that a triplet state lies only 130 $cm^{-1}$ in energy above it. This triplet state has the same composition as the lowest energy triplet state observed by Dedieu et al.[18] in ab initio SCF calculations. These results strongly support the observation of a paramagnetic contribution to the observed magnetic susceptibility. Thus, for the case of thermal equilibrium at 20 °C, our calculations predict approximately a 1:3 occupancy of the lowest excited triplet state relative to the diamagnetic ground state. In fact, the calculated separation of 130 $cm^{-1}$ between the lowest excited triplet state and the diamagnetic ground state agrees completely with the energy difference deduced empirically by Cerdonio et al.[4,6] by fitting the observed temperature dependence of the magnetic susceptibility for oxyhemoglobin. Although Cerdonio and co-workers fit their measured susceptibility as a function of $1/T$ by assuming thermal equilibrium between an antiferromagnetic singlet state and a ferromagnetic triplet state lying 146 $cm^{-1}$ above the singlet state, it is possible to fit the observed magnetic behavior equally well by assuming thermal equilibrium between a diamagnetic ground state and an excited triplet state. The configuration-interaction results described here, which place the lowest antiferromagnetic singlet state involving substantial $d\pi \rightarrow O\pi^*$ character at 13 500 $cm^{-1}$ above the diamagnetic ground state, indicate that the latter of these two possibilities is the correct one. Such a low-lying triplet also has relevance for the iron $K_\beta$ fluorescence emission spectrum of oxyhemoglobin.[47]

Our results strongly imply that INDO-type SCF calculations with empirical parametrization provide a more reliable description of the electronic ground state of oxyheme than do the results of theoretical parametrization or ab initio SCF results. Only the empirically parametrized INDO calculations yield a ground state having a large negative electric field gradient with the principal component in the heme plane ($V_{xx}$), in very good agreement with experimental results for single-crystal Mössbauer resonance of oxymyoglobin regarding sign, anisotropy, magnitude, and direction of the largest tensor component of the electric field gradient.[26,27] Further, the empirically parametrized INDO results suggest ferric superoxide character, while both the ab initio results of Dedieu et al.[18] and the theoretically parametrized INDO results for model oxyheme investigated in this work predict a ferrous–neutral dioxygen bond. Similar findings have been reported by Rohmer and Loew[35] for the case of oxy-P450.

As seen in Table IV, the origin of the ferric superoxide character comes from extensive electron delocalization. There is an appreciable amount of back-bonding from the iron atom to the dioxygen ligand. Specifically, the iron $d_{yz}$ orbital donates approximately one electron to the oxygen $\pi_g^*$ orbital. In turn, in forward donation the formally empty iron $d_{z^2}$ and $d_{xy}$ orbitals receive approximately one electron from the porphyrin and imidazole $\sigma$ orbitals. Furthermore, approximately half an electron is transferred to the iron s and p orbitals via delocalization. This accounts for the atomic charges of 1.41 on the iron atom and −0.75 on the dioxygen ligand, as reported in Table III. These large covalent effects cause a significant deviation from the spherical symmetry of the low-spin ferrous configuration $(d_{x^2-y^2})^2(d_{xz})^2(d_{yz})^2$, resulting in the anomalously large electric field gradient observed.

The large temperature dependence of the quadrupole splitting observed in the model oxyheme compound could be accounted for by rotational averaging about the Fe–O bond (Table VI). A much smaller temperature dependence, consistent with observation in the intact protein, is obtained by a restricted averaging over only a 45° range of values for the $C_{22}$–Fe–O–O torsion angle.

A fourfold, symmetric barrier of about 7 kcal/mol is calculated for rotation of the terminal oxygen atom about the Fe–O bond. The minimum-energy conformers ($\phi = 0$, 90, 180, 270°) all correspond to the terminal oxygen bisecting the $N_{pyr}$–Fe–$N_{pyr}$ bond angles. The maxima correspond in two instances ($\phi = 67.5$ and 247.5°) to the terminal oxygen eclipsed with the imidazole ligand, but the other two maxima correspond to the symmetric positions ($\phi = 157.5$ and 337.5°) in which the imidazole is not directly below the $O_2$ ligand. The value of 7 kcal/mol obtained without geometry relaxation is an upper limit to this rotational barrier. The fact that this barrier is almost completely symmetric indicates that there is no explicit trans effect due to the imidazole ligand on the other side of the porphyrin plane.

Ab initio calculations[16-18] on two of the conformations of a five-coordinated ferrous oxyporphyrin with $\phi = 0$ and 45°

yielded an energy difference of 5.6 kcal/mol with the larger energy at $\phi = 45°$. From Figure 3, we find an energy difference of about 3 kcal/mol between these conformers ($\phi = 0, 45°$). Loew and Kirchner[48] report a rotational barrier of less than 5 kcal/mol from an iterative extended Hückel calculation on model oxyheme. The relatively low barrier to rotation reported in this work is consistent with the fourfold statistical disorder of the dioxygen ligand observed for the dioxygen complex of the picket-fence porphyrin.[39]

## Conclusions

The results of the configuration-interaction calculations on model oxyheme definitively establish a diamagnetic ground state with a very low-lying triplet state (129 $cm^{-1}$) and an "antiferromagnetic" singlet of much higher energy (13 500 $cm^{-1}$) above it. Thus, they provide a simple rationale for the temperature-dependent magnetic susceptibility observed for oxyhemoglobin: namely, thermal equilibrium between a diamagnetic ground state and a paramagnetic excited triplet state lying very close in energy to the ground state. The efficacy of the empirical parametrization in INDO for yielding a good description of the ground state of model oxyheme is demonstrated by the excellent agreement between the calculated and experimental electric field gradient. The aspherical charge distribution on the iron atom corresponding to a $Fe^{III}(d^5)$–$O_2^-$ complex is consistent with the anomalously large electric field gradient. Finally, the relatively low barrier to rotation calculated for the dioxygen ligand is in accord with the statistical disorder observed in the crystal structure of model oxyheme.

**Acknowledgments.** This research was initiated while one of us (Z.S.H.) was a guest at the Quantum Chemistry Group at the University of Uppsala, Sweden. He wishes to thank Professor Per-Olov Löwdin for his gracious hospitality and Professor Michael Zerner for initiating him into the subtleties of his INDO-CI program. Helpful discussions with Dr. Marie-Madeleine Rohmer are gratefully acknowledged. This research was supported by National Science Foundation Grant PCM 7921591.

## References and Notes

(1) L. Pauling and C. D. Coryell, *Proc. Natl. Acad. Sci. U.S.A.*, **22**, 210 (1936).
(2) C. D. Coryell, L. Pauling, and R. W. Dodson, *J. Phys. Chem.*, **43**, 825 (1939).
(3) D. S. Taylor and C. D. Coryell, *J. Am. Chem. Soc.*, **60**, 1177 (1938).
(4) M. Cerdonio, A. Congiu-Castellano, F. Mogno, B. Pispisa, G. L. Romani, and S. Vitale, *Proc. Natl. Acad. Sci. U.S.A.*, **74**, 398 (1977).
(5) L. Pauling, *Proc. Natl. Acad. Sci. U.S.A.*, **74**, 2612 (1977).
(6) M. Cerdonio, A. Congiu-Castellano, L. Calabrese, S. Morante, B. Pispisa, and S. Vitale, *Proc. Natl. Acad. Sci. U.S.A.*, **75**, 4916 (1978).
(7) J. J. Weiss, *Nature (London)*, **202**, 83 (1964).
(8) J. J. Weiss, *Nature (London)*, **203**, 183 (1964).
(9) J. B. Wittenberg, B. A. Wittenberg, J. Peisach, and W. E. Blumberg, *Proc. Natl. Acad. Sci. U.S.A.*, **67**, 1846 (1970).
(10) J. P. Collman, J. I. Brauman, T. R. Halbert, and K. S. Suslick, *Proc. Natl. Acad. Sci. U.S.A.*, **73**, 3333 (1975).
(11) G. Lang and W. Marshall, *Proc. Phys. Soc., London*, **87**, 3 (1966).
(12) L. Pauling, "Hemoglobin", Butterworths, London, 1949, p 57.
(13) M. Zerner, M. Gouterman, and H. Kobayashi, *Theor. Chim. Acta*, **6**, 363 (1966).
(14) B. B. Wayland, J. V. Minkiewicz, and M. E. Abd-Elmageed, *J. Am. Chem. Soc.*, **96**, 2795 (1974).
(15) W. A. Goddard III and B. D. Olafson, *Proc. Natl. Acad. Sci. U.S.A.*, **72**, 2335 (1975).
(16) A. Dedieu, M. M. Rohmer, M. Bernard, and A. Veillard, *J. Am. Chem. Soc.*, **98**, 3717 (1976).
(17) A. Dedieu, M. M. Rohmer, H. Veillard, and A. Veillard, *Bull. Soc. Chim. Belg.*, **85**, 953 (1976).
(18) A. Dedieu, M. M. Rohmer, and A. Veillard in "Metal-Ligand Interactions in Organic Chemistry and Biochemistry", Part 2, B. Pullman and N. Goldblum, Eds., D. Reidel Publishing Co., Dordrecht, Holland, 1977, pp 101–130.
(19) R. F. Kirchner and G. H. Loew, *J. Am. Chem. Soc.*, **99**, 4637 (1977).
(20) G. H. Loew and R. F. Kirchner, *Int. J. Quantum Chem., Quantum Biol. Symp.*, **5**, 403 (1978).
(21) B. H. Huynh, D. A. Case, and M. Karplus, *J. Am. Chem. Soc.*, **99**, 6103 (1977).
(22) D. A. Case, B. H. Huynk, and M. Karplus, *J. Am. Chem. Soc.*, **101**, 4433 (1979).
(23) W. A. Eaton, L. K. Hanson, P. J. Stephens, J. C. Sutherland, and J. B. R. Dunn, *J. Am. Chem. Soc.*, **100**, 4991 (1978).
(24) M. W. Makinen, A. K. Churg, and H. A. Glick, *Proc. Natl. Acad. Sci. U.S.A.*, **75**, 2291 (1978).
(25) J. A. Pople and D. L. Beveridge, "Approximate Molecular Orbital Theory", McGraw-Hill, New York, 1970.
(26) K. Spartalian, G. Lang, J. P. Collman, R. R. Gagne, and C. A. Reed, *J. Chem. Phys.*, **63**, 5375 (1975).
(27) Y. Maeda, T. Harami, Y. Morita, A. Trautwein, and U. Gonser, presented at the Sixth International Biophysics Congress, Kyoto, Japan, Sept 3–9, 1978.
(28) J. P. Collman, R. R. Gagne, C. A. Reed, T. R. Halbert, G. Lang, and W. T. Robinson, *J. Am. Chem. Soc.*, **97**, 1427 (1975).
(29) G. B. Jameson, G. A. Rodley, W. T. Robinson, R. R. Gagne, C. A. Reed, and J. P. Collman, *Inorg. Chem.*, **17**, 850 (1978).
(30) J. P. Collman, *Acc. Chem. Res.*, **10**, 265 (1977).
(31) J. Ridley and M. Zerner, *Theor. Chim. Acta*, **32**, 111 (1973).
(32) J. Ridley and M. Zerner, *Theor. Chim. Acta*, **42**, 223 (1976).
(33) A. D. Bacon, Ph.D. Thesis, University of Guelph, 1976.
(34) A. D. Bacon and M. C. Zerner, *Theor. Chim. Acta*, **53**, 21 (1979).
(35) M. M. Rohmer and G. H. Loew, *Int. J. Quantum Chem., Quantum Biol. Symp.*, in press.
(36) M. C. Zerner, G. H. Loew, R. F. Kirchner, and U. T. Mueller-Westerhoff, *J. Am. Chem. Soc.*, in press.
(37) K. Weiss, unpublished.
(38) N. Mataga and K. Nishimoto, *Z. Phys. Chem. (Frankfurt am Main)*, **13**, 140 (1957).
(39) J. P. Collman, R. R. Gagne, C. A. Reed, W. T. Robinson, and G. A. Rodley, *Proc. Natl. Acad. Sci. U.S.A.*, **71**, 1326 (1974).
(40) L. Pauling, *Nature (London)*, **203**, 182 (1964).
(41) J. S. Griffith, *Proc. R. Soc. London, Ser. A*, **235**, 23 (1956).
(42) R. S. Mulliken, *J. Chem. Phys.*, **23**, 1833, 2338, 2343 (1955).
(43) A. K. Churg and M. W. Makinen, *J. Chem. Phys.*, **68**, 1913 (1978).
(44) G. H. Loew, Z. S. Herman, and M. C. Zerner, *Int. J. Quantum Chem.*, in press.
(45) S. N. Ray, T. Lee, R. P. Das, R. M. Sternheimer, R. P. Gupta, and S. K. Sen, *Phys. Rev. A*, **11**, 1804 (1975).
(46) E. J. Heidner, R. C. Ladner, and M. F. Perutz, *J. Mol. Biol.*, **104**, 707 (1976).
(47) A. S. Koster, *J. Chem. Phys.*, **63**, 3284 (1975).
(48) G. H. Loew and R. F. Kirchner, *J. Am. Chem. Soc.*, **97**, 7388 (1975).